Quarter-Salt Formation Defining the Anomalous Temperature Dependence of the Aqueous Solubility of Sodium Monododecyl Phosphate

ARTICLE *in* THE JOURNAL OF PHYSICAL CHEMISTRY B · JANUARY 2007

Impact Factor: 3.3 · DOI: 10.1021/jp062731c · Source: PubMed

2 AUTHORS:

Joseph Carnali
Unilever
24 PUBLICATIONS **374** CITATIONS
SEE PROFILE

Brian A Pethica
Princeton University
169 PUBLICATIONS **3,608** CITATIONS
SEE PROFILE

Quarter-Salt Formation Defining the Anomalous Temperature Dependence of the Aqueous Solubility of Sodium Monododecyl Phosphate

Joseph O. Carnali*

Unilever Research and Development, 40 Merritt Boulevard, Trumbull, Connecticut 06611

Brian A. Pethica

Department of Chemical Engineering, Princeton University, Princeton, New Jersey 08544

Received: May 4, 2006; In Final Form: October 3, 2006

The salts of monoalkyl phosphates (MAPs) have been identified as a class of inherently mild surfactants for use in household and personal products. They represent an anionic species intermediate in terms of pK_a between the sulfates and the carboxylates and are analogous to the carboxylates in that they form acid-salts (which are here termed quarter-salts)—hydrogen-bonded dimers consisting of an undissociated MAP acid and an MAP monosalt. These complexes precipitate from solutions of the monosalt over a range of lower MAP concentrations giving rise to an unusual solubility/temperature relationship. The solubility of monosodium monododecyl phosphate ($NaC_{12}MAP$) increases with temperature up to 0.01 M at ∼60 °C, which corresponds to the conventional Krafft point as shown by the appearance of micelles in solution. The solubility then increases further to ∼0.04 M as the solubility temperature declines from 60 to 38 °C. The transition between these two trends is characterized by a rather sharp temperature maximum in the solubility curve. In a third stage, the solubility then rises rapidly with very small change of temperature. This unusual overall behavior is shown to correspond with three distinct solid-phase compositions for the precipitates at temperatures below the solubility curve. At the lowest concentrations and up through the Krafft Point, the solid phase has been identified as the stoichiometric quarter-salt. Over the declining temperature portion of the solubility curve, the supernatant solution coexists with a macroscopic mixture of separate quarter-salt and monosalt solids. In the high-concentration third region the solid phase is exclusively the MAP monosalt. The coprecipitation of quarter-salt and monosalt from the monosalt solution occurs reversibly in the declining portion of the solubility curve and is accompanied by an increase in pH. The four phase system (solution, vapor, and two pure solid phases) retains one degree of freedom according to the phase rule since the system is in effect three component in that region.

Introduction

Surfactants used in household and personal products are frequently in contact with human skin, with a potential for skin irritation or roughness.[1] Many factors contribute to irritation, including defatting of skin lipids, surfactant binding to skin proteins followed by denaturation, and surfactant permeability in skin.[2] Reducing this potential for irritation is an active field of technology,[3] and a common approach has been to search for milder surfactants. The monosalts of the monoalkyl phosphates (MAPs) with the general structure

$$C_nH_{2n+1}PO_4H^-X^+$$

(where X^+ is an univalent cation) comprise one such class, as shown by Imokawa and colleagues,[4] who demonstrated that the monosodium salt of *n*-dodecyl phosphate ester (which is here designated as $NaC_{12}MAP$) was only 1/10 as irritating as sodium dodecyl sulfate.

Alkyl phosphates represent an intermediate class of anionic surfactant, between the weakly ionized carboxyl of soaps and the fully ionized sulfates.[5−7] The first and second pK_a's of monododecyl phosphoric acid in water were estimated as 2−3 and 7.0, respectively, by Pethica et al.[5,8] The insolubility of the MAP acid in water makes it difficult to determine the first end point accurately.[9]

The phenomenon of acid-salt formation in alkyl phosphate systems has been known since Brown et al.[10] prepared the so-called "quarter-salts" by adding 0.25 equiv of NaOH to alkyl dihydrogen phosphates in ethanol and isolating the products. X-ray diffraction analysis of the quarter-salts showed a pattern of short spacings which was distinctly different from that of either the $NaC_{12}MAP$ (monosodium alkyl hydrogen phosphate) or the unneutralized acid. It has been noted that monoalkyl phosphate salts in nonpolar solvent solution form hexamers and higher aggregates.[11] Insoluble monolayers of monobehenyl phosphate were studied by Hunt,[11] who found evidence for the formation of a stable quarter-salt dimer at pH 4.1. The ratio of phosphate to potassium ion was determined as approximately 2/1, confirming that, of the four acid hydrogen atoms of the dimer, only one is replaced by the alkali metal. This compound was found to be very stable, even in the presence of dilute mineral acid. Muller et al.[12] studied monohexadecyl phosphate monolayers and also postulated dimers in which strong hydrogen bonding occurred between the ionized oxygen of one phosphate group and the hydroxyl hydrogen of a nearest neighbor. Walde

* Corresponding author. E-mail: joseph.carnali@unilever.com. Tel: 203-381-5444. Fax: 203-381-5487.

10.1021/jp062731c CCC: $33.50
Published on Web 11/22/2006

et al.[9] noted spontaneous vesicle formation in quarter-salts prepared by using 50 mM citric acid as buffer. Interaction between the monosalt and the acid via hydrogen bonding is believed to provide the appropriate head group size and curvature for vesicles.

The relevance of the quarter-salt complex to the aqueous solution properties of MAPs was first suggested by Imokawa et al.,[1] who determined the solubility/temperature relationship of NaC_{12}MAP and NaC_{16}MAP. The solubility temperature was shown to increase with surfactant concentration, as expected, up to a maximum at 0.01 M phosphate, and then decreased with further increase in surfactant concentration up to 0.04 M. The latter trend is not typical of anionic surfactants,[6] and it was proposed that, in dilute solution, some of the monosodium salt undergoes partial hydrolysis to give a bimolecular aggregate between disodium salt and unneutralized monoalkyl phosphate. Arakawa and Pethica[8] also noted a change in sign of the temperature coefficient of the solubility of monopotassium decyl and dodecyl phosphates. Referencing Brown et al.,[10] these authors attributed the anomaly to hydrolysis of the alkyl phosphate to form the quarter-salt:

$$2RPO_4H^-Na^+ \rightleftharpoons RPO_4H^-Na^+ \cdot RPO_4H_2 + Na^+ + OH^- \quad (1)$$

The maximum temperature in the solubility-temperature curve was taken as the apparent Krafft point, since micelles were demonstrated in solutions at and above this point and for all solutions at temperatures above the solubility line with concentrations above 0.01 M. The quarter-salts are stable in the solid phase and will precipitate on addition of acid. The formation of the quarter-salt from NaC_{12}MAP in solution yields a rise in pH, as indicated in eq 1.

It should be noted that the MAP quarter-salt system is in some ways analogous to the acid soap phenomenon which itself has been extensively studied for over 100 years.[13,14] The acid soaps are fixed stoichiometric ratio complexes formed between a fatty acid and an alkali soap due to strong hydrogen bonding between the headgroups and coordination to a common cation.[15] Their occurrence has sometimes been ignored in the interest of presenting a generalized picture of surfactant phase behavior[6] — much of the early work in soap systems was conducted in dilute alkali to suppress any hydrolysis.[6,16,17] However, the details of the hydrolysis were well studied by Powney and Jordan,[18] who observed that the extent of hydrolysis was in the range of 5−15% at 10^{-2}−10^{-3} M for a range of soap chain lengths. Early attempts to describe the observed hydrolysis behavior quantitatively in terms of fatty acid complexation and then fatty acid incorporation into soap micelles[19] proved incomplete, and a more satisfactory treatment is that of Lucassen[20] which considers the coequilibria of solid fatty acid and/or solid fatty acid soap and/or solid soap with aqueous solution.

In this work, the aqueous solubility and solution properties of NaC_{12}MAP are studied as a function of temperature and concentration. The unusual reversal of the trend of the solubility temperature with increasing concentration is again observed. New to this study is an analysis of the solids which precipitate along the solubility curve. This solid phase is not simply the monosalt at all temperatures, as would be the case for a typical sulfate or sulfonate surfactant. Rather, the nature of the solid phase varies with the total NaC_{12}MAP level and temperature. The solid precipitated at the lower concentrations and below the Krafft Point temperature consists of the quarter-salt. In the declining temperature stage, the solids comprise a mixture of the quarter-salt and the monosalt NaC_{12}MAP. At the highest total concentrations studied, the precipitate is simply the monosalt MAP. The progression in the chemistry of the precipitated solids as the MAP concentration increases is shown to account for the form of the solubility curve.

Materials and Methods

Materials. Commercial alkyl phosphates are typically mixtures of mono-, di-, and trialkyl esters.[9,21,22] The monododecyl phosphate used in this work was kindly donated by Kao Corp. (Chemicals Division, Tokyo, Japan) as a high-purity commercial sample, MAP-20H. This material was further purified by first recrystallizing the acid two times from isooctane, followed by air drying and then vacuum drying at room temperature.[9] The purity of the resulting product was checked by a number of techniques, including ^{1}H NMR, elemental analysis, and potentiometric titration.

The mono-/diester ratio of the purified MAP acid, as well as any possible presence of residual inorganic phosphoric acid, was determined via potentiometric titration of the MAP solution in 65/35 v/v ethanol/water with and without silver nitrate, following the procedure of Kurosaki et al.[23] and Schmitt.[24] An accurately weighed sample of the MAP acid to be analyzed was titrated with 0.1 M NaOH, showing two inflection points at pH 5.5 and 10.0. The monoester contributes to both potentiometric breaks, but the diester contributes only to the first inflection. Thus, a second equivalence point which is less than twice the first is an indication of diester impurity. To isolate any contribution of phosphoric acid, a second titration is performed on another sample of identical weight. After the first inflection point, sufficient silver nitrate is added to precipitate all the free phosphate ions. Any phosphoric acid will combine with silver nitrate to form the yellow precipitate of silver phosphate, according to

$$NaH_2PO_4 + 3AgNO_3 = Ag_3PO_4 + NaNO_3 + 2HNO_3 \quad (2)$$

The titration is continued until the usual second inflection point, which will be at a higher titer than that observed in the absence of silver nitrate because of the third proton from phosphoric acid which is released as HNO_3. Thus, the difference between the second equivalence point with and without silver nitrate is the number of moles of free phosphoric acid. Neither diester nor phosphoric acid could be detected in the purified acid sample.

An independent check on the mono-/diester ratio was made by first synthesizing the triethanol ammonium salt of MAP via neutralization of the MAP acid in ethanolic solution with triethanolamine and then recrystalizing twice from ethanol. The ^{1}H NMR of this salt, in D_2O, gave integrated peak areas for the $O-CH_2$, $N-CH_2$, and methyl/methylene protons in the ratio of 8.1/6.0/24.0, respectively, versus the expected 8/6/23. Elemental analysis of the MAP acid was performed by Schwarzkopf Microanalytical Laboratory, Inc. (Woodside, NY). For the MAP acid, the findings were C, 54.02%, H, 10.32%, and P, 11.22%, versus the expected levels C, 54.1%, H, 10.2%, and P, 11.6%. The melting point for the acid was found to be 58 °C, in agreement with that reported by Nakagaki et al.[25] Last, the chain-length distribution of the starting alcohol was characterized by the procedure of Tsuji and Konishi[24,26] in which the MAP acid is decomposed with acetic acid and *para*-toluenesulfonic anhydride. The volatile acetate ester was analyzed by gas chromatography, using the referenced procedure[26] modified to run on an Agilent 6890 Plus gas chromatograph equipped with a flame ionization detector and using

helium as the carrier gas. Compared with a parallel chromatograph of standard *n*-alkanol derivatives, the present MAP sample gave greater than 97% of the expected peak area at a retention time equivalent to dodecanol.

The NaC_{12}MAP was prepared from the MAP acid in boiling ethanol by adding dropwise a stoichiometric equiv of 2 N NaOH solution (Fisher).[1] It was necessary to add a small quantity of water to the solution during the course of the alkali addition in order to keep the monosalt which forms in solution. The NaC_{12}-MAP precipitated upon cooling and was filtered off, recrystallized again, and then dried under vacuum over P_2O_5. Elemental analysis again confirmed the purity of this material. To aid in the interpretation of the IR spectra of the MAP quarter-salt, a synthetic quarter-salt sample was prepared by adding 50% of the NaOH required for monosalt formation to a boiling ethanolic solution of MAP acid. The solid isolated upon cooling was twice recrystallized and dried. As a further assistance, a quarter-salt sample was prepared in which the phosphate P−OH proton was substituted with deuterium (P−OD). To prepare this sample, use was made of the fact that appropriately dilute NaC_{12}MAP solutions, heated to above the Krafft point, developed a precipitate upon cooling which consisted essentially of the anhydrous quarter-salt (see below). Thus the 0.01 M (0.33%) NaC_{12}MAP sample, prepared in 99.95% D_2O, precipitated with the exchangeable hydroxyl proton replaced with deuterium. The solid collected was then equilibrated over a saturated solution of potassium acetate in D_2O (22% relative humidity) to maintain the exchanged deuterium.

Solubility Curve Measurements. Varying amounts of solid surfactant were weighed into screw-top vials, followed by gravimetric addition of Milli-Q water (18.2 MΩ cm). The water was freshly boiled to reduce the level of dissolved CO_2, and a few sets of samples were also prepared under a nitrogen atmosphere—neither of these precautions affected the results. The sealed vials where then placed in a thermostated water bath whose temperature was first set to 5 °C, to ensure that a solid phase was present in each case. Visual observations of the sample turbidity were then made as the bath temperature was increased in 1 °C intervals with 30 min equilibration times. For a given surfactant concentration, the first temperature at which the sample became transparent, with no suspended crystals, defined the solubility boundary. For repetitive measurement of the same samples, the completely solubilized MAP solutions were cooled overnight to room temperature and then further cooled to 5 °C until all samples showed the presence of a precipitate. Stepwise heating was again employed, and the reoccurrence of the crystal dissolution was observed with a reproducibility of ±1 °C.

The presence of micelles in the NaC_{12}MAP solutions as a function of temperature and total NaC_{12}MAP level was determined via solubilization of the hydrophobic dye Orange OT.[27,28] A dye level of 0.2% was sufficient to saturate all the systems studied, regardless of the NaC_{12}MAP level, and the samples were heated to above the Krafft point and held there for several hours until they developed a constant color intensity. The amount of solubilized dye at the elevated temperature was gauged from the absorbance measured at 423 nm on a HP 8453 spectrophotometer. The absorbance data were found to be independent of the number of heating/cooling cycles to which the samples were subjected.

Analysis of Solid-Phase Components. Systems heated to above the Krafft point were allowed to cool overnight to room temperature and invariably formed a precipitate. The pH of the clear supernatant solution was determined, but the systems were left to equilibrate for a further 1−2 days before the solids were isolated by filtration using a 0.22 μm filter. The filtrates were washed with a small amount of ice water, placed into individual weighing bottles, and then stored first over Drierite and then over P_2O_5 under vacuum until they reached constant weight. Thermogravimetric analysis (Perkin-Elmer TGA 7) revealed that the dry materials showed no weight loss until 150 °C, at which temperature decomposition began to occur.

Thermal analysis of the isolated solids was performed on a TA Instruments 2920 modulated DSC using a dual sample cell with an empty pan as the reference. Samples of 4−7 mg mass were sealed in aluminum pans and equilibrated at 0 °C for 5 min before being ramped to 130 °C at 5 °C/min. After cooling of the samples at the same rate back to 0 °C, the heating ramp was then repeated. Transition temperatures were determined by extrapolating the slope of any endotherm onset to the baseline. Enthalpies were measured from the area under the transition peak by comparison with areas of a known standard (indium).

The solid phase was also studied using a Nicolet Magna-IR 750 FT-IR spectrophotometer using a DTGS detector and a DRIFTS accessory (Spectra Tech Inc.). The sample was ground to a powder and diluted with spectroscopic grade KBr. Each spectrum represents the signal average of 32 scans taken at 8 cm^{-1} resolution, and a background correction has been made by subtracting the contribution from the KBr. Interference in the spectra resulting from water and CO_2 residues in the IR apparatus was eliminated by purging with dry nitrogen. Polarized microscopy was performed using a Nikon Eclipse 6600 equipped with a Linkam TMS 94 hot stage.

Small-angle X-ray diffraction (SAXS) measurements were carried out using a Microsource X-ray generator operating at 45 kW and 0.66 mA. The Cu Kα X-ray beam is focused with Confocal Max-Flux optics and passes in vacuum through the sample, which is loaded into a stainless steel cell equipped with thin mica windows. The scattered intensity is recorded on a 2-D position sensitive proportional counter manufactured by Molecular Metrology. Before measurements, Q values were calibrated with silver behenate (here $Q = (4\pi/\lambda) \sin \theta$ is the scattering vector, λ and θ being the X-ray wavelength and scattering angle, respectively).

The composition of the solids was determined in terms of the ratio of MAP acid to NaC_{12}MAP monosalt. This determination was made in three ways. First, samples were analyzed for their phosphate and sodium content by Schwarzkopf Microanalytical Laboratory. Second, a known weight of the solid was dissolved in 50/50 ethanol water and then titrated potentiometrically with 0.1 M NaOH to the second end point.[29] Assuming that the solid is a mixture of MAP acid (molecular weight 266) and NaC_{12}MAP (molecular weight 288), the weight fraction of the acid form can be calculated from

$$\text{acid weight fraction} = (m - y/288)/(4.0466 \times 10^{-3} y) \quad (3)$$

where m is the number of moles of titrant employed and y is the sample weight in grams.

Third, the ratio of MAP acid to monosalt was determined from the relative magnitudes of the endotherms characteristic of the quarter-salt and monosalt species. It was then assumed, on the basis of the data in Figure 1a, that the measured enthalpy in the region of the endotherm at 75 °C was due entirely to the NaC_{12}MAP component of the sample expressed as

$$\Delta H_{ms} = \Delta h_1 X_1 w \quad (4)$$

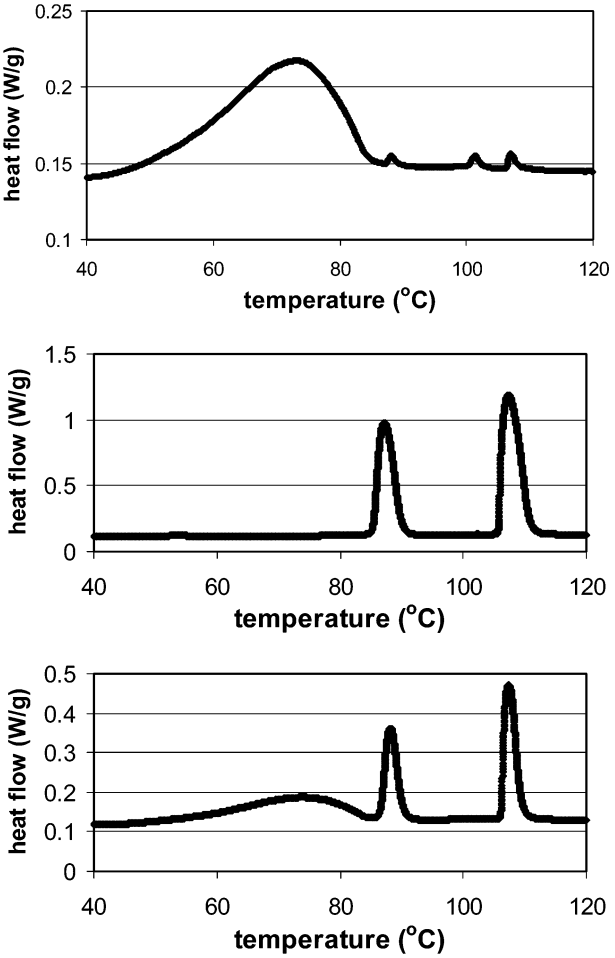

Figure 1. DSC heating curves obtained at a 5 °C min^{-1} scanning rate for (top to bottom) (a) anhydrous $NaC_{12}MAP$, (b) dry solids from 0.007 M (0.2%) solids sample, and (c) dry solids from 0.034 M (1%) solids sample.

where Δh_1 is the enthalpy/gram of the monosalt at this temperature (18 J/g), X_1 is the weight fraction of monosalt in the sample, and w is the sample weight. For the quarter-salt, the sharp endothermic peaks at 86 or 106 °C (Figure 1b) were assumed characteristic and the weight fractions of this species, X_2, calculated from

$$\Delta H_{ms} = \Delta h_2 X_2 w \quad (5)$$

Here the enthalpies/gram for the quarter-salt were taken as Δh_2 = 30.7 J/g (86 °C) and 42.8 J/g (106 °C).

As a precaution, the precipitated material was checked for the possible occurrence of ester hydrolysis back to fatty alcohol as discussed by Kurosaki et al.[23,30] A sample which precipitated as the monosalt was dispersed in 50/50 ethanol/water and then extracted five times with petroleum ether, the collected ether phase being evaporated off. The amount of extracted material determined gravimetrically, which would be dodecanol if hydrolysis occurred, was immeasurably small. This finding is in agreement with Tahara et al.[31] and Arakawa and Pethica,[8] who both found negligible ester hydrolysis of alkyl phosphates in aqueous solutions.

Results

Solubility Curve. The solubility of $NaC_{12}MAP$ as a function of temperature shows the interesting trend reported in Figure 2a. At the lowest total concentrations shown, increasing MAP

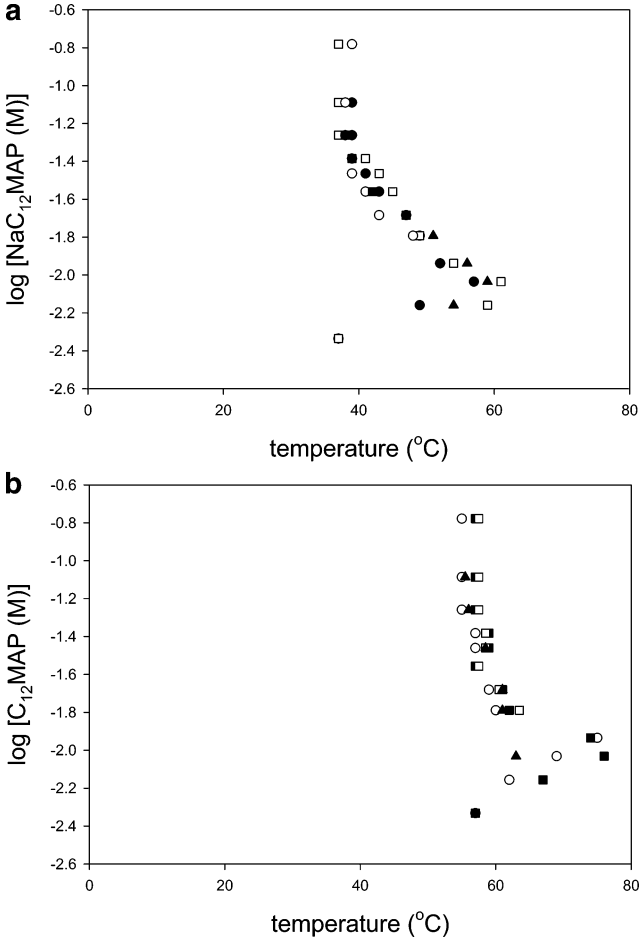

Figure 2. (a) Solubility of $NaC_{12}MAP$ as a function of temperature. Solutions are isotropic to the right of the boundary (see text), except for a Tyndall color present at the peak temperature of the curve, occurring at about 0.01 M. Symbols indicate repeated determinations. (b) Solubility curve for the 90% NaMAP/10% MAP acid system. The concentration scale gives the total concentration of MAP (monosalt plus acid). A Tyndall color is present at the peak temperature of the curve, occurring at about 0.01 M. Symbols indicate repeated determinations.

levels require higher temperatures for complete dissolution. For a MAP concentration in the vicinity of 0.01 M (0.3 wt %), the dissolution temperature reaches a maximum, with the last crystals disappearing in the temperature interval 59−61 °C. The solution retained a faint Tyndall color at this point which persisted to higher temperatures. Higher $NaC_{12}MAP$ concentrations then showed a reverse trend in that the temperature for full solubilization decreased with increasing total $NaC_{12}MAP$ level over the range 0.01−0.04 M (0.3 − 1%) and then assumed a constant value of about 38 °C for higher concentrations. The final solutions were completely clear for temperatures above the solubility boundary indicated in Figure 2a, except for the one exception noted above.

In a parallel study, the solubility of a mixture of 90 wt % $NaC_{12}MAP$ and 10 wt % MAP acid was determined. This system will be referred to as 90%/10%, and the prior one, as 100%/0%. The immediate effect of this partial acid substitution (see Figure 2b) is an elevation of the solubilization temperature. The temperature plateau at higher MAP levels now occurs at about 58 °C, and this plateau replaces the region of declining solubility temperature with increasing concentration that occurred over the 0.01−0.04 M (0.3−1%) interval in the absence of added MAP acid. The dissolution temperature still reaches a maximum in the vicinity of 0.01 M (0.3 wt %) MAP, but it is

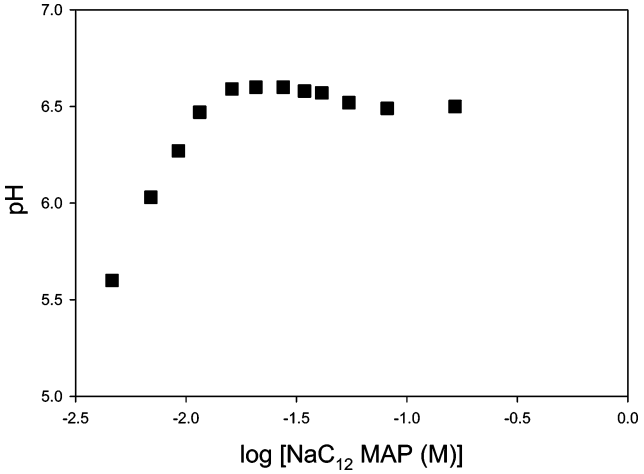

Figure 3. pH in the supernatant phase of the $NaC_{12}MAP$ solutions after heating to above the Krafft point and then standing overnight at room temperature. Uncertainty in the measurements is reflected in the size of the symbols.

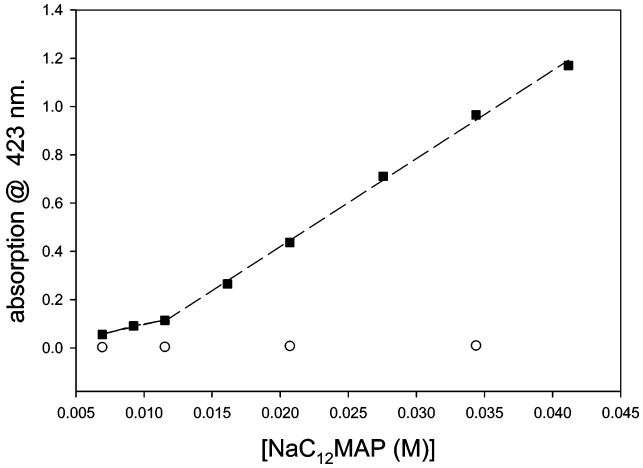

Figure 4. Absorbance measured at 423 nm of $NaC_{12}MAP$ systems of varying total concentration, each with excess solid dye (0.2% Orange OT). Samples equilibrated at 60 °C (filled square symbols) were isotropic solutions, and those at 25 °C (open circles) contained precipitated solids.

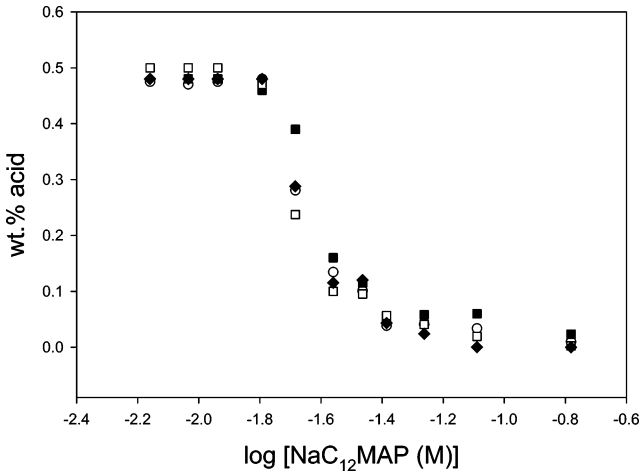

Figure 5. Chemical composition of the solid phases isolated from the $NaC_{12}MAP$ solutions upon cooling from above the Krafft point to room temperature. The solids are assumed to be mixtures of MAP acid and MAP monosalt. Symbols indicate the different determination techniques employed: open circles, ratio of sample quarter-salt endotherm to that of pure quarter-salt; closed squares, chemical analysis of sodium; open squares, titration with dilute alkali; closed diamonds, ratio of sample salt endotherm to that of pure monosalt.

difficult to determine the true dissolution temperature as the solution retains a faint Tyndall color at this concentration even up to 80 °C. At lower concentrations of the 90%/10% mixture the dissolution temperature declines with decreasing concentration.

Figure 3 records the measured pH in the supernatant phase of systems heated to above the Krafft point and then cooled to room temperature and held overnight. Over the concentration range studied, the pH rises with increasing bulk concentration from a low of about 5.6 and then shows a plateau of about 6.6 at intermediate concentrations before falling off slightly to a second plateau at the highest concentration studied. The increase in pH with concentration can be understood in terms of the hydrolysis described in eq 1. The released NaOH will be buffered by conversion of monosalt to disalt, so that quantitative interpretation of the pH measurements is not straightforward. The first plateau pH region is of interest because it occurs over the concentration range in which both the quarter-salt and the monosalt are present as solid phases (see below).

A series of $NaC_{12}MAP$ samples, spanning the same range of surfactant concentration as explored in Figure 2, was saturated with Orange OT and heated to above the Krafft point. The color intensity measured at 423 nm increased with $NaC_{12}MAP$ level, as shown in Figure 4, and was characterized by two linear regions intersecting at approximately 0.01 M $NaC_{12}MAP$. The linear region to higher concentrations extended up to the highest MAP levels studied and is interpreted as indicating a linearly increasing number of micelles which each solubilize the same amount of dye.[9] The linear region to lower concentration is interpreted as a premicellar region, so that the critical micelle concentration is determined by this technique to be 0.01 ± 0.002 M at 60 °C. This value can be compared with the cmc of KC_{12}-MAP at 55 °C, measured as 0.0094 M by Arakawa and Pethica.[8] Thus, $NaC_{12}MAP$ systems form true micellar solutions above the Krafft point. In a parallel study, the Orange OT was not added until the samples cooled to room temperature and a precipitate formed. In this case, the absorbance was the same as that found in the control (dispersion of dye in water), confirming the absence of micelles below the solubility curve.

Solid-Phase Composition. The composition of the solid phase precipitated at room temperature was determined as shown in Figure 5 for the 100%/0% $NaC_{12}MAP$ system. The three experimental techniques used to determine the weight percentage of MAP acid in the quarter-salt/monosalt mixture were all found to be in good agreement. The shape of the curve of weight fraction acid versus total MAP level shows a progression as the concentration rises from a quarter-salt precipitate to a monosalt precipitate through a region of intermediate composition. The precipitated phase has a composition of about 48% MAP diacid, as would be expected of the quarter-salt, up to approximately 0.016 M (0.5%) total MAP. Beyond about 0.05 M (1.5%), the precipitate is composed entirely of $NaC_{12}MAP$. In between these two boundary levels, the precipitate isolated has a varying composition, with an acid fraction which decreases smoothly with increasing total $NaC_{12}MAP$ level.

The isolated solid phases were dehydrated prior to chemical analysis for simplicity of interpretation. To estimate their water content upon precipitation, a selection of the solid samples were rehydrated over saturated salt solutions of various relative humidity (RH). The monosalt remains anhydrous up through 64% RH but picks up 12% water at 75% RH (saturated NaCl) and then 3% more for a total of 15% water at 84% RH (saturated KCl). This mass of water corresponds to 2.4 water molecules

per NaC_{12}MAP. The behavior of the MAP monosalt can be contrasted with the long-chain sodium soaps, whose crystals seem to swell smoothly with increasing humidity.[16] The quarter-salt forms no stable hydrates up to 91% RH ($BaCl_2$), as is similarly observed for acid soaps.[32,33]

The composition of the supernatant solution over the precipitate at room temperature was also determined for a few samples by potentiometric titration. At the highest NaC_{12}MAP level studied, the supernatant was evaporated to dryness, showing that it had a solids content of 0.23%. Titration of this solid indicated that the material was all NaC_{12}MAP. A sample from the quarter-salt region (0.01 M, 0.33% MAP) was similarly dried down to indicate a 0.23% solids solution. Titration of this solid, interpreted as if it were all monosalt, indicated that the supernatant had a monosalt level of 0.18%. The difference between the solids interpreted as monosalt and the total solids can be explained in terms of the NaOH formed during hydrolysis which will convert a fraction of the MAP to disalt.

Thermal Analysis. The DSC up-curve for C_{12}MAP acid (not shown) displayed a melting endotherm at 59 °C with an onset temperature of 57 °C and a heat of melting of 128.5 J/g. Anhydrous C_{12}NaMAP (Figure 1a) displays a broad endotherm with an onset temperature of about 55 °C, centered at about 75 °C and with an enthalpy of 18 J/g. The precipitated solids isolated from samples of the 100%/0% system at the Krafft point show a completely different thermal pattern, with two sharp endotherms at around 86 and 106 °C and corresponding enthalpies of 30.7 and 42.8 J/g, respectively (Figure 1b). The same DSC scan is observed from the synthetic quarter-salt (see above). In all cases, the endotherms in Figure 1 were fully reversible (heating versus cooling) with peak shapes which did not change upon reducing the rate to 1 °C/min. Solids from the samples in the region of the solubility curve where the solubilization temperature decreased with increasing total MAP level showed both the broad endotherm at 75 °C and the two sharper endotherms at 86 and 106 °C (see Figure 1c). The shape and transition temperature of these endotherms did not change throughout this region. However, the relative ratio of the enthalpy at 75 °C to that at 86 °C (or equivalently that at 106 °C) did increase smoothly on passing from the peak at the Krafft point, where there is no 75 °C endotherm, down to the plateau, where there are no 86 and 106 °C endotherms. This observed behavior was the basis for the use of eqs 4 and 5 to estimate the composition of the precipitated phase. Thermal analysis of solids isolated from the 90%/10% system (not shown) display the same trends—except for the presence of the 86 and 106 °C endotherms—for all samples studied.

The dried NaC_{12}MAP solid, which showed a broad endotherm with onset temperature of 55 °C and peak at 75 °C, was studied further by hot-stage polarized microscopy and small-angle X-ray diffraction. Microscopy showed the monosalt to be a weakly birefringent crystal whose platelike, trapezoidal habit did not change as the temperature was ramped up through the endothermic transition detected by DSC. Moreover, the sample remained a free flowing powder. SAXS of the material at room temperature showed a lamellar crystal structure with a single long spacing at 35.7 Å and the corresponding second-order reflection. The molecular origin of the weak NaC_{12}MAP solid transition might be related to the freezing of headgroup rotation which has been observed on the NMR time scale in vesicles made with dialkyl MAPs.[34]

SAXS studies on the quarter-salt gave evidence for an lamellar packing with a long spacing of 34.5 Å. The finding of a long spacing for the monosalt which is larger than that of the quarter-salt is in agreement with the work of Brown et al.[10] Hot-stage microscopy of this material showed it to occur as platelike trapezoidal crystals which were strongly birefringent, relative to those of the salt. This birefringence was observed to be reduced (but not eliminated) in an abrupt fashion upon heating to the 86 °C transition observed in DSC. The material remained a free flowing powder throughout the temperature range studied. This finding is reasonable in that the enthalpy of melting of 1:1 potassium hydrogen dioleate acid-soap crystals was determined by Cistola et al.[35] to be 126 J/g. In the dodecanoic acid/K dodecanoate system, incongruent melting of the acid soap was observed at around 100 °C with an enthalpy of 135.6 J/g, resulting in a dispersion of solid soap in molten acid.[29] The smaller endotherms observed here must thus be premelting transitions. In comparison again to the acid soaps, the above dodecanoic/dodecanoate acid soap shows a transition prior to incongruent melting with an energy of about 44 J/g [36] — comparable to the transition energies reported here.

Infrared Spectroscopy. Systematic studies of phosphate compounds and full assignment of their vibrational spectra are relatively rare. Further, such assignments are difficult, particularly in the 900−1200 cm^{-1} range, due to the high degree of coupling between the vibrational modes.[37] On the basis of a consultation with the literature,[38,39] we tentatively assign the MAP spectra plotted in Figure 6 as follows. The peak at 2954−2955 cm^{-1} is attributed to the CH_3 asymmetric and symmetric stretching bands, while the CH_2 asymmetric and symmetric stretching appear at 2918−2919 and 2850−2852 cm^{-1}, respectively.[40,41] These peak positions vary by no more than ±1 cm^{-1} over the range of samples shown in Figure 6: MAP acid (Figure 6a); NaC_{12}MAP (Figure 6b); synthetic quarter-salt (Figure 6c); in-situ samples (Figure 6d−f; see below). A broad band, appearing at approximately 2350−2380 cm^{-1}, can be assigned to the H−O stretching and bending vibration in P(═O)O−H. In the solid MAP acid, synthetic quarter-salt, and NaC_{12}MAP, the species exist as dimers (or higher order complexes) involving O−H···O hydrogen bonds. This band should thus be attributed to vibrational modes of the coupled O−H bonds. As would be expected, this band is missing from the spectrum of MAP di Na salt (not shown),[38,39] a species which cannot complex with itself via hydrogen bonding. In the order from the acid, to NaC_{12}-MAP, to synthetic quarter-salt, the location of this band shifts from 2322 cm^{-1} to 2350 cm^{-1} to 2380 cm^{-1}, respectively, indicating a progressive strengthening of the hydrogen bond.

There are several bands in the region 980−1250 cm^{-1} due to the phosphate group.[12] The MAP acid has an absorption band in the region 1240 cm^{-1}, corresponding to stretching mode vibrations of the phosphoryl group (P═O).[39,42] The major resonance at 1033 cm^{-1} is assigned to the stretching vibration of the P−O bond of the P−O−C and P−O−H groups.[38,40,41] The weak peak at 982 cm^{-1} can be attributed to the P−OH stretching vibration. The NaC_{12}MAP (monosalt) shows some distinct differences. The P═O stretching mode vibrations are shifted to slightly higher wavenumbers and split away from the P−O stretch, which also moves from 1033 to 1087 cm^{-1}. The other major change is the P−OH stretch which moves down in wavenumber from 982 to 926 cm^{-1} and grows in intensity. The synthetic quarter-salt is further dominated by this peak, now at 960 cm^{-1}. Comparison with the synthetic quarter-salt prepared in a D_2O environment showed that this peak shifted roughly 27 cm^{-1} lower in frequency upon changing P−OH to P−OD, thus providing further evidence for this assignment of the resonance.[43] The in situ samples, precipitated solids isolated from samples at 0.01 M (0.33%), 0.02 M (0.6%), and 0.05 M

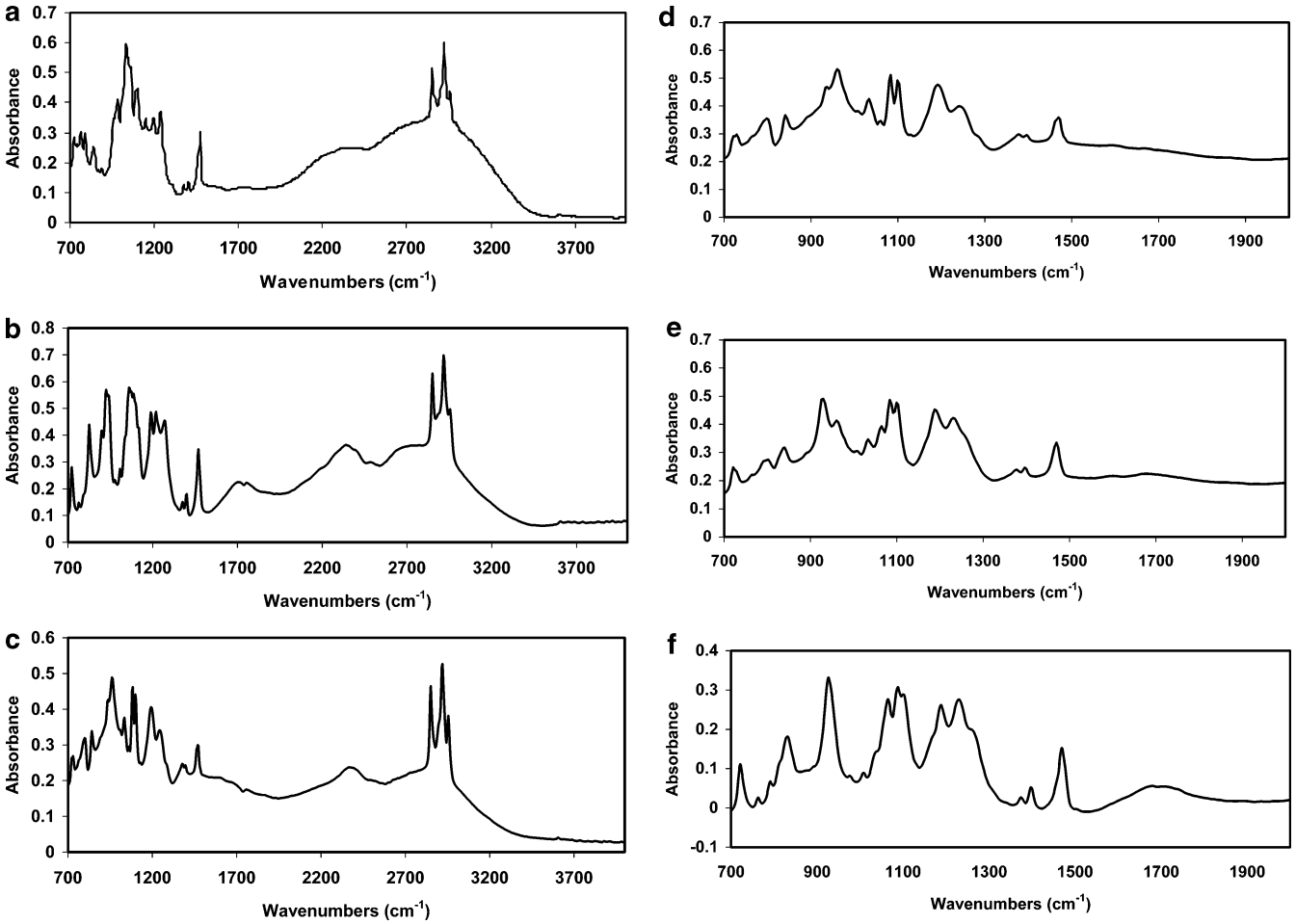

Figure 6. IR spectra of solids: (a) MAP acid; (b) NaC_{12}MAP; (c) quarter-salt. Dry solids are from (d) in-situ 0.01 M (0.33%), (e) in-situ 0.02 M (0.6%), and (f) in-situ 0.055 M (1.6%).

(1.6%) NaC_{12}MAP, show evidence for the superposition of the monosalt and quarter-salt spectra in this region, with absorption peaks at 926 and 960 cm^{-1}, respectively. For the quarter-salt-rich 0.01 M sample (Figure 6d), the 960 cm^{-1} line dominates while the 926 cm^{-1} line is prominent for the monosalt-rich 0.05 M sample (Figure 6f). For the 0.02 M sample (Figure 6e), which is roughly half-and-half monosalt and quarter-salt, the intensities of these two bands are approximately equal.

Discussion

Nature of the Mixed Solids Region. The region of the solubility curve in which the solubilization temperature decreases with increasing NaC_{12}MAP overall concentration is characterized by the presence of a precipitated phase whose composition is reported in Figure 5. This composition varies smoothly between 100% quarter-salt at the Krafft point to pure monosalt at the beginning of the range of high concentrations characterized by an almost constant solubilization temperature (plateau). The DSC and IR results indicate that the precipitates formed in this region consist of separate coexisting crystals of the quarter-salt and of NaC_{12}MAP. Solid solutions of these two species can be ruled out. Prior workers in pharmaceuticals[44] and paraffins[45−47] have distinguished between solid solutions and crystal mixtures on the basis of the fact that crystal mixtures display thermograms which are superpositions of the individual species while solid solutions show new transitions at temperatures which move smoothly between those of the pure components as the bulk ratio varies. Similarities between the crystal structures and between the shapes and sizes of the component molecules are typical requirements for solid solution formation. The quarter-salt and the monosalt do not show such obvious physical similarities, and solid solutions in the analogous acid soap and soap system have not been reported.[20] As was noted in the Results, the shape and transition temperatures of the endotherms characteristic of the quarter-salt and monosalt, respectively, are unchanged on going from the quarter-salt- or monosalt-only regions to the region where both species are present. This observation precludes the occurrence of crystals of solid solutions of mixed quarter-salt and NaC_{12}MAP and supports the conclusion that pure quarter-salt and pure monosalt crystals are both present in the mixed region. The good agreement of the macroscopic composition data derived from titration and elemental analysis with that of thermal analysis via eqs 4 and 5 also supports this conclusion. The IR results are in agreement with this above picture in that the mixed solids region shows a superposition of the spectra of pure quarter-salt and monosalt species. The relative weighting of the two components in the spectra changes in proportion to the bulk composition as described in Figure 5.

As additional and direct evidence, polarized light microscopy was used to examine the crystals isolated from the mixed solids region. As was noted in the Results, the pure quarter-salt crystals were more strongly birefringent than those of the salt. In the mixed solids regions, strongly and weakly birefringent crystals were observed to be randomly mixed. Figure 7a shows a typical side-by-side pair of such crystals (center of figure) in a bright field image. Under crossed polarization, Figure 7b, the right-hand crystal (monosalt) essentially disappears while the left-

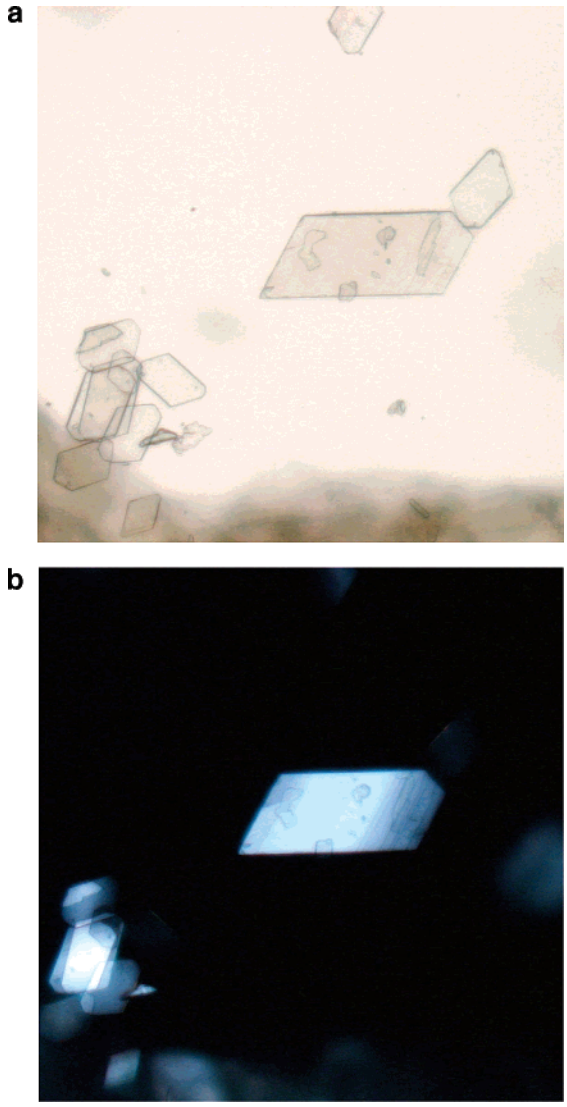

Figure 7. Images at 100× magnification of dried crystals isolated from the mixed solids region. The first photomicrograph is a bright-field image, and the second is the image observed through crossed polarizers. Note that some of the crystals are strongly birefringent while others essentially disappear under polarization.

hand crystal (quarter-salt) is quite visible. Upon heating of this sample on the hot stage, the quarter-salt crystal showed a reduction in birefringence at about 86 °C, as would be expected. Thus, the precipitate composition variation is found to be due to a physical mixture of two crystals whose ratio varies smoothly from all quarter-salt at the lower total composition boundary to all NaC_{12}MAP at the higher total composition boundary. Solid solutions are ruled out.

Application of the Phase Rule. The phase rule is traditionally stated as

$$F = C - P + 2 \tag{6}$$

in which C represents the number of components in the system, P is the number of phases present, and F is the number of degrees of freedom—the number of intensive variables to be specified to determine the state of the system.[48] Simply on the basis of the number of chemical species used to prepare the samples, the present system would be considered binary, with water and NaC_{12}MAP as components. Adopting $C = 2$ would lead to $F = 0$ (an invariance point) for our system when it contains four phases (two solids, one liquid, and one vapor).

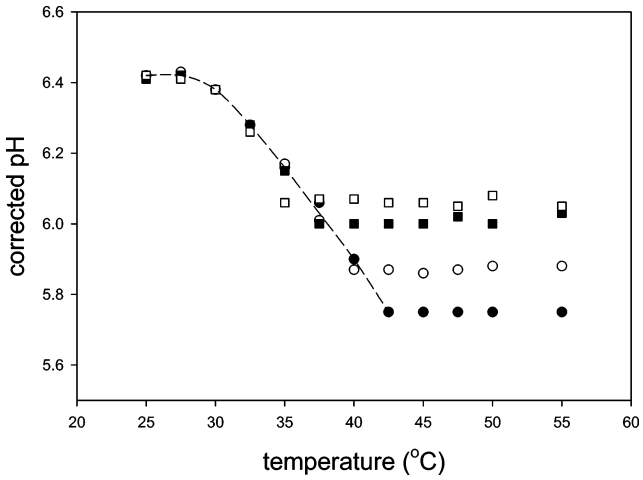

Figure 8. pH of a series of NaC_{12}MAP solutions, with total concentrations spanning the two solid-phase regions. Solutions were cooled from above the Krafft point. Appearance of the solid phases begins where the solution temperature meets the dashed line. Key to symbols: 0.016 M, filled circles; 0.02 M, open circles; 0.028 M, filled squares; 0.034 M, open squares.

This is contrary to the results shown in Figures 2a and 8 and to other aspects of the experimental evidence. When the solute ionizes or forms a reaction product with the solvent in the two-phase system of water and NaC_{12}MAP in solution in equilibrium with water vapor, the variance remains at two since additional constraints are introduced by the ionization and reaction equilibria between the several chemical species in solution. However, when a reaction product can form a distinct solid phase, its separation does not reduce the variance since the composition of the residual solution phase depends on the extent of the precipitate, requiring specification of an extra compositional variable for the solution phase to complete the statement of variance. A good example of this requirement is given by Zemansky[49] for the case of the formation of a precipitate of aluminum hydroxide from aqueous solutions of aluminum chloride. This viewpoint has also been stated by Ricci[48] as applicable to any salt/water binary systems in which the salt can hydrolyze and form a separate solid phase and has been specifically invoked for the analogous fatty acid soap system by Laughlin[6] and by Cistola et al.[50] It follows that, for the region of the NaC_{12}MAP/water system in which two solid phases occur, the system has four phases and three phase-rule-defined components, giving a variance of one, in accordance with the data. For the region in which only NaC_{12}MAP is present in the solid state, there are two components and the variance is one. For the region in which only the quarter salt is present as a solid phase, the variance is two. In a formal analysis of the reaction and ionization equilibria, possible choices of the third component (taking water and the MAP monosalt as the first two) when solid quarter-salt is present include the hydrogen ion via measurements of pH.

Phase rule considerations in traditional soap/water systems (for example, sodium palmitate), explicitly taking hydrolysis into account, have been discussed by Lucassen.[20] The situation of two solid phases, either fatty acid and acid soap or acid soap and soap, coexisting with a supernatant solution at constant temperature and pressure requires that the solution composition be fixed. This situation is analogous to a binary system in a three-phase region (including vapor) at constant temperature and pressure, where there is no influence of bulk composition on the phase behavior, except insofar as the volume fraction of the constant composition phases is concerned.

The data heretofore presented do not allow a detailed check for adherence to the phase rule. The pH plateau in the two-solid-phase region of Figure 3, however, suggested the following study. Samples at bulk Na C_{12}MAP concentrations spanning this region (at room temperature) were heated to above the Krafft point to yield isotropic solutions. They were then cooled in incremental steps of 2.5 °C and the pH measured at each step after a time period of 30 min. The pH data presented in Figure 8 have been corrected for temperature effects using standardized buffers. In isotropic solutions, the pH increases with NaC_{12}-MAP concentration but stays constant as the temperature is lowered at a given concentration. When the temperature reaches the precipitation point (e.g. at about 40 °C, for the 0.016 M (0.46%) case) precipitation begins and the pH rises appreciably. This observation has also been reported by Arakawa and Pethica.[8] With decreasing temperature, the amount of precipitated material increases and the pH rises along the dotted line in Figure 8. This line is shared for all the initial concentrations in the two-solid region and is an expression of the one degree of freedom predicted from the phase rule. The solution concentration at the phase boundary at a given temperature is known, and the composition of the solution phases is accessible from the reaction equilibrium relation for the hydrolysis if the pH is also measured. Thus, the system is fully defined in terms of the phase rule. The observation that the number of condensed phases changes with increasing NaC_{12}MAP concentration: quarter-salt plus solution to quarter-salt plus monosalt plus solution to monosalt plus solution, or two to three to two, is also in keeping with the alteration rule,[6] another aspect of adherence to the phase rule.

Semiquantitative Description of the Solubility Curve. The phenomena reported in Figure 2a are in agreement with the findings of Imokawa et al.,[1] who reported a retreat of the solubility temperature with increasing concentration for Na C_{12}-MAP concentrations below about 0.03 M, and with the findings of Arakawa and Pethica,[8] who noticed the same phenomena in the vicinity of 0.01 M for KC_{12}MAP. The solubility curve determined in this study can now be discussed in more detail, considering, in sequence, the very low concentration region, the region of the maximum in temperature, the region in which the solution temperature declines with increasing concentration, and the region of rapidly increasing concentration at almost constant temperature.

In the low-concentration region, the solubility of the NaC_{12}-MAP is found to increase with temperature as is typical of sulfate and sulfonate surfactants. Solid quarter-salt is formed along the solubility curve up through the Krafft point. Thus, although NaC_{12}MAP is the compound added to the solution, its dissolution leads to the attainment of the solubility product for the quarter-salt, which then defines this portion of the solubility curve. Direct evidence for this process comes from rapidly cooling samples from above the solubility curve in this concentration region. Rapid cooling by immersion in an ice/salt bath at −10 °C resulted in a precipitate whose composition (as gauged by the relative magnitudes of the characteristic endotherms) was over 80 wt % NaC_{12}MAP. Such rapid cooling creates a large supersaturation for both the quarter-salt and the monosalt, but the kinetic complexity of quarter-salt formation is not believed to favor precipitation of this species unless it already exists in solution. The observation of monosalt during rapid cooling indicates that it is this species which is present above the solubility curve. A similar mechanism, requiring a soap solubility only on the order of 10^{-5} M, has been proposed for acid soap systems.[32]

At 0.01 M (0.33%) total MAP, separate experiments were performed in which the equivalent amount of synthetic quarter-salt, as found in Figure 5, was combined with the appropriate amount of monosalt and water and heated. Crystals were still present for any temperature below 57 °C, as expected from the results in Figure 2a, but the crystals disappeared at about 60 °C and the samples developed a Tyndall color. A separate DSC study of damp, synthetic quarter-salt crystals shows that an endothermic melting transition occurs at 59 °C. In the case of the 0.01 M NaC_{12} MAP, heating to above 59 °C results in a melt which dispersed into the aqueous phase to give the Tyndall color observed at the peak of the solubility curve. This behavior is again a manifestation of the solubility product of the quarter-salt but at this concentration occurs above the melting point of the species. The behavior of the damp crystal differs from that of the quarter-salt in the absence of water, which has no melting transition below 120 °C. This reduction in the temperature of crystal thermal transitions in the presence of solvent is frequently observed.[6]

In the region where the solubility temperature retreats with increasing total NaC_{12}MAP level, the solid phase below the curve consists of mixed crystals of quarter-salt and monosalt. Thus, the solubility products of the quarter-salt (which can, by extension of the work of Lucassen,[20] be written as $K_{QS} = [H^+][Na^+][C_{12}PO_4H^-]^2$) and the monosalt simultaneously control this portion of the solubility curve. Also in this region, micelles are detected at and above the temperature traced by the solubility curve, as shown by Orange OT solubilization. It is believed that micelle formation, acting to control the monomer concentration $[C_{12}PO_4H^-]$, combines with the temperature dependence of the solubility products to define the retreat of the solubility temperature. The dissolution of the quarter-salt is seen as the reverse of the step studied in Figure 8 and corresponds to a drop in the pH with increment in temperature as monosalt re-forms and dissolves. Further direct evidence that the dissolution process does not result in a soluble quarter-salt species comes again from cooling samples in this concentration region from above the Krafft point at various cooling rates. Rapid cooling by immersion in an ice/salt bath resulted in a precipitate which was practically devoid of quarter-salt. As noted above, rapid cooling is not believed to favor precipitation of the quarter-salt unless it already exists in solution, and the observation of monosalt exclusively indicates that this is the only species present above the Krafft point.

In the high-concentration, temperature-plateau region, the solid phase below the solubility curve is NaC_{12}MAP. This material displays traditional surfactant behavior with a solubility which changes rapidly with temperature, due to the formation of micelles at temperatures at and above the solubility curve. The unusual features of the NaC_{12}MAP solubility curve thus correspond to the occurrence of the two−three−two condensed phase coexistence.

The behavior of the 90%/10% system helps to clarify some of the above points. While the quarter-salt found in the 100%/0% system converts back into soluble salt species at temperatures generally below the melting point of the quarter-salt, the higher levels of quarter-salt present in the 90%/10% system require going to higher temperature to satisfy the solubility product. The quarter-salt melts at this higher temperature, giving the extended range of Tyndall color observed. Further, the added MAP acid ensures that the quarter-salt solubility product is always relevant, so that a concentration region where only NaC_{12}MAP precipitates (as in the 100%/0% system) is not observed. Prior studies of the solubility phenomena in phosphate

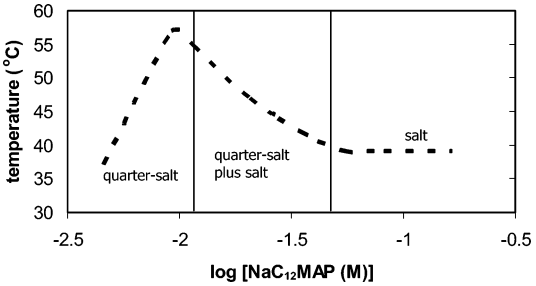

Figure 9. Schematic diagram showing the solubility curve for NaC_{12}-MAP and indicating the solid phase(s) in equilibrium with the aqueous solution at room temperature.

systems have postulated quarter-salt solubilization inside of monosalt micelles as the mechanism for dissolution.[1,8] While this mechanism cannot be ruled out by the present observations, it does not appear to be necessary to invoke a separate process beyond the solubility criteria. A schematic diagram illustrating the key features of the solubility curve for the 100%/0% system, with the corresponding solid phases with which it is in equilibrium, is shown in Figure 9.

The analogy of these results with the fatty acid soap system has been noted by previous authors.[8,9] The formation of intermediate species such as the quarter-salt for the straight chain sulfate and sulfonates has at least been suggested by Rao.[7] Such intermediates are able to perform the dual roles of collector and frother in flotation applications. For the fatty acid soaps, the formation of the acid soap can be observed during titration of the fatty acid with alkali or of the soap with mineral acid.[51] In these titrations it is observed that the acid soap species is most noticeable at "high" soap concentration (greater than about 10^{-2} M). However, in the study of the solubility curve of long chain soaps, acid soap precipitation was found to occur at the lowest concentrations studied.[16] A comprehensive theoretical picture was presented by Lucassen,[20] but experimental verification of the solid phases formed has not, to our knowledge, been pursued. The NaC_{12}MAP system appears to be somewhat easier to study than the comparable soap system—providing a relatively large amount of precipitated solids for analysis. It will be of interest to adapt Lucassen's treatment to the MAP system and to then compare with experimental data in a future publication.

Conclusions

Aqueous solutions of monosodium monododecyl phosphate (NaC_{12}MAP) exhibit an anomalous solubility−temperature relationship showing three characteristic regions. At low concentrations, the solubility increases with temperature up to ~0.01 M at ~60 °C at which micelles are first formed. Beyond this point the solubility increases to ~0.04 M as the solubility temperature declines to ~38 °C, beyond which the solubility increases rapidly with little change in temperature. The solid phases coexisting with the supernatants in these three regions have been identified by titration analysis, scanning calorimetry, X-ray crystallography, IR spectroscopy, and polarization microscopy. It is shown that the unusual solubility properties can be explained by the formation of a quarter-salt which can crystallize from solution. The quarter salt forms the coexisting solid phase in the low-concentration region of the solubility curve. In the region of declining solubility temperature with increase in concentration, the coexisting solids consist of a mixture of separate crystals of the quarter-salt and of the NaC_{12}-MAP itself. At the highest concentrations, the coexisting solid phase is NaC_{12}MAP alone. Application of the phase rule shows that the number of components is three when the quarter-salt occurs in the solid phase and two when the solid phase consists of NaC_{12}MAP alone. This situation leads to a variance of two along the solubility curve at low concentrations and one along the curve for both the region of declining solubility temperature and in the highest concentration region at near-constant temperature.

Acknowledgment. It is a pleasure to thank Mr. Dane Drutis for help with the infrared spectroscopy, Mr. Pravin Shah for his advice concerning several aspects of the chemical analysis, and Dr. Qiang Qiu for performing the SAXS work. We also thank Unilever Research and Development for allowing us to publish this work. One of the reviewers for this paper is acknowledged for his thought-provoking questions.

Supporting Information Available: SAXS pattern for anhydrous NaC_{12}MAP. This material is available free of charge via the Internet at http://pubs.acs.org

References and Notes

(1) Imokawa, G.; Tsutsumi, H.; Kurosaki, T. *J. Am. Oil Chem. Soc.* **1978**, *55*, 839.
(2) Imokawa, G. *J. Am. Oil Chem. Soc.* **1979**, *56*, 604.
(3) Ananthapadmanabhan, K. P.; Subramanyan, K.; Nole, G. In *Dry skin and moisturizers, chemistry and function*, 2nd ed.; Lodén, M., Maibach, H. I., Eds.; Taylor & Francis: New York, 2006.
(4) Imokawa, G. *J. Soc. Cosmet. Chem.* **1980**, *31*, 45.
(5) Parreira, H. C.; Pethica, B. A. In *Gas/Liquid and Liquid/Liquid Interfaces, Proceedings of the Second International Congress on Surface Activity*; Butterworths: London, 1957.
(6) Laughlin, R. G. *The aqueous phase behavior of surfactants*; Academic Press: London, 1994.
(7) Rao, S. R. *Surface chemistry of froth flotation*, 2nd ed.; Kluwer Academic/Plenum Publishers: New York, 2004.
(8) Arakawa, J.; Pethica, B. A. *J. Colloid Interface Sci.* **1980**, *75*, 441.
(9) Walde, P.; Wessicken, M.; Rädler, U.; Berclaz, N.; Conde-Frieboes, K.; Luisi, P. L. *J. Phys. Chem. B* **1997**, *101*, 7390.
(10) Brown, D. A.; Malkin, T.; Maliphant, G. K. *J. Chem. Soc.* **1956**, 1584.
(11) Hunt, E. C. *J. Colloid Interface Science* **1969**, *29*, 105.
(12) Müller, H.; Friberg, S.; Hellsten, M. *J. Colloid Interface Sci.* **1970**, *32*, 132.
(13) Chevreul, M. E. *On the Chemical Study of Animal Fat*; Paris, 1823.
(14) Zhu, S.; Heppenstall-Butler, M.; Butler, M. F.; Pudney, P. D. A.; Ferdinando, D.; Mutch, K. J. *J. Phys. Chem. B* **2005**, *109*, 11753.
(15) Lynch, M. L.; Wireko, F.; Tarek, M.; Klein, M. *J. Phys. Chem. B* **2001**, *105*, 552.
(16) de Mul, M. N. G.; Davis, H. T.; Evans, D. F.; Aparna, A. V.; Wagner, J. R. *Langmuir* **2000**, *16*, 8276.
(17) Oginol, K.; Ichikawa, Y. *Bull. Chem. Soc. Jpn.* **1976**, *49*, 2683.
(18) Powney, J.; Jordan, D. O. *Trans. Faraday Soc.* **1938**, *34*, 363.
(19) Stainsby, G.; Alexander, A. E *Trans. Faraday Soc.* **1949**, *45*, 585.
(20) Lucassen, J. *J. Phys. Chem.* **1966**, *70*, 1824.
(21) Cooper, R. S. *J. Am. Oil Chem. Soc.* **1963**, *40*, 642.
(22) Miller, D.; Wiener, E. -M.; Turowski, A.; Thunig, C.; Hoffmann, H. *Colloids Surf., A* **1999**, *152*, 155.
(23) Kurosaki, T.; Wakatsuki, J.; Imamura, T.; Matsunaga, A.; Furugaki, H.; Sassa, Y. *Comun. Jorn. Com. Esp. Deterg.* **1988**, *19*, 191.
(24) Schmitt, T. M. *Analysis of surfactants*; Marcel Dekker: New York, 1992.
(25) Nakagaki, M.; Handa, T.; Shimabayashi, S. *J. Colloid Interface Sci.* **1973**, *43*, 521.
(26) Tsuji, K.; Konishi, K. *J. Am. Oil Chem. Soc.* **1975**, *52*, 106.
(27) Adamson, A. W. *Physical chemistry of surfaces*, 3rd ed.; Wiley: New York, 1976.
(28) Namani, T.; Walde, P. *Langmuir* **2005**, *21*, 6210.
(29) Goddard, E. D.; Goldwasser, S.; Golikeri, G.; Kung, H. C. *Adv. Chem. Ser.* **1968**, *No. 84*, 67.
(30) Bunton, C. A. *J. Chem. Educ.* **1968**, *45*, 21.
(31) Tahara, T.; Satake, I.; Matuura, R. *Bull. Chem. Soc. Jpn.* **1969**, *42*, 1201.
(32) Lynch, M. L. *Curr. Opin. Colloid Interface Sci.* **1997**, *2*, 495.
(33) Mantsch, H. H.; Weng, S. F.; Yang, P. W;. Eysel, H. H. *J. Mol. Struct.* **1994**, *324*, 133.
(34) Wagenaar, A.; Streefland, L.; Hoekstra, D.; Engberts, J. B. F. N. *J. Phys. Org. Chem.* **1992,** *5*, 451.

(35) Cistola, D. P.; Atkinson, D.; Hamilton, J. A.; Small, D. M. *Biochemistry* **1986**, *25*, 2804.
(36) Kung, H. C.; Goddard, E. D. *J. Colloid Interface Sci.* **1969**, *29*, 242.
(37) Carauta, A. N. M.; de Souza, V.; Hollauer, E.; Téllez S., C. A. *Spectrochim. Acta, Part A* **2004**, *60*, 41.
(38) Song, X.; Sun, S.; Zhang, W.; Yin, Z. *J. Colloid Interface Sci.* **2004**, *272*, 463.
(39) Vorsina, I. A.; Levich, I. S. *Russ. J. Inorg. Chem.* **1967**, *12*, 1612.
(40) Sheng, Y.; Zhou, B.; Zhao, J.; Tao, N.; Yu, K.; Tian, Y.; Wang, Z.-C. *J. Colloid Interface Sci.* **2004**, *272*, 326.
(41) Tanaka, H.; Watanabe, T.; Chikazawa, M.; Kandori, K.; Ishikawa, T. *Colloids Surfaces, A* **1998**, *139*, 341.
(42) Rumyantseva, N. M.; Smyalkovskaya, E. N.; Gusev, A. A.;. Khar'kov, S. N. *Zh. Prikl. Khim.* **1979**, *52*, 2216.
(43) Tanaka, H.; Oomori, K.; Hino, R. *J. Colloid Interface Sci.* **2004**, *273*, 685.
(44) Nie, Q.; Gong, J. B.; Wang, J. K.; Wang, S. *Ind. Eng. Chem. Res.* **2006**, *45*, 432.
(45) Coutinho, J. A. P.; Ruffier-Mèray, V. *Ind. Eng. Chem. Res.* **1997**, *36*, 4977.
(46) Yamamoto, H.; Nemoto, N.; Tashiro, K. *J. Phys. Chem. B* **2004**, *108*, 5827.
(47) Guo, X.; Pethica, B. A.; Huang, J. S.; Prud'homme, R. K. *Macromolecules* **2004**, *37*, 5638.
(48) Ricci, J. E. *The phase rule and heterogeneous equilibrium*; Van Nostrand: New York, 1951.
(49) Zemansky, M. W. *Heat and thermodynamics*, 3rd ed.; McGraw-Hill: New York, 1951.
(50) Cistola, D. P.; Hamilton, J. A.; Jackson, D.; Small, D. *Biochemistry* **1988**, *27*, 1881.
(51) Rosano, H. L.; Breindel, K.; Schulman, J.; Eydt, A. J. *J. Colloid Interface Sci.* **1966**, *22*, 58.